Galaxy Zoo-CANDELS : Bar Fractions from $0.5 < z < 2^\star$

Simmons, Melvin, Lintott, Masters, Keel, Willett, Rutkowski, Schawinski, Smethurst, Cheung, (need authors for UDS redshifts), GZ, CANDELS, et al.; name order still in flux

[1] *Oxford Astrophysics, Denys Wilkinson Building, Keble Road, Oxford OX1 3RH, UK*

20 January 2014

ABSTRACT

The formation of bars in disks is a tracer of the dynamical maturity of disk galaxies. At $z > 1$, it is expected that dynamically mature disks are rare. Here we report the discovery of barred structures in massive disk galaxies at $z \sim 1.5$ in deep rest-frame optical images from CANDELS. From within a sample of 876 disk galaxies identified by visual classification in Galaxy Zoo, we identify 123 barred galaxies (a fraction $f_{bar} = 14\%$). Selecting a sub-sample within the same region (brighter than L^*) of the evolving galaxy luminosity function, which allows for more direct comparison to previous studies and alleviates possible bias effects due to surface brightness dimming, we find that the bar fraction does not evolve across the redshift range $0.5 \leqslant z \leqslant 2$. We discuss the implications of this discovery in the context of existing simulations and our current understanding of the way disk galaxies have evolved over the last 11 billion years.

Key words:
galaxies: bars — galaxies: evolution — galaxies: general — galaxies: spiral

1 INTRODUCTION

Because galactic stellar bars form only within dynamically cold, rotationally supported disks (Athanassoula 2005; Combes 2009; Sellwood 2010; Athanassoula et al. 2013), the evolution of the fraction of disk galaxies with bar features traces the overall evolution of disk galaxy dynamics. Locally, bars are present in $\sim 25 - 50\%$ of disk galaxies (e.g. Masters et al. 2011; Aguerri et al. 2009), with their abundance steadily decreasing to $\sim$10% of disk galaxies at $z \sim 1$ (Elmegreen et al. 2004; Elmegreen & Elmegreen 2005; Sheth et al. 2008; Melvin et al. 2013).

The lower incidence of bars at higher redshifts may be in part be due to the increased incidence of mergers and galaxy interactions (Conselice et al. 2003; Lotz et al. 2011), which disrupt and heat disks. It may also be related to the expected increase in disk gas fraction with redshift (observed indirectly via the increase in specific star formation rate to $z \sim 2$, e.g., Lilly et al. 1996, Madau et al. 1998, and directly via **anyone? (?)**), a quantity with which bars are observed to be anti-correlated (Masters et al. 2012) in

agreement with theoretical predictions (Friedli & Benz 1993; Berentzen et al. 2007; Villa-Vargas et al. 2010; Athanassoula et al. 2013, though a high gas fraction does not entirely preclude the existence of a bar; Nair & Abraham 2010; Masters et al. 2012).

The current theoretical understanding of bar fraction evolution suggests that disk galaxies with $z > 1$ are too dynamically hot to become unstable to bar formation (e.g., Kraljic, Bournaud, & Martig 2012 predict no observable bars within their simulated sample at $z \sim 1.5$). Other simulations explore the impact of tidal heating and galaxy harassment, which can either inhibit bar formation *or* promote it, depending on mass (with higher-mass galaxies being more likely to form a long-lasting bar due to a minor merger or interaction; Moore et al. 1996; Skibba et al. 2012). Testing this requires high-resolution imaging over large areas to observe statistically significant samples with sufficient Δz resolution to observe evolution and adequate spatial resolution to resolve galactic-scale bars in the rest-frame optical (since the detectability of bars decreases rapidly blueward of the 4000 Å break).

These observing requirements currently limit studies of disk populations via bar fractions to surveys with the *Hubble Space Telescope (HST)*. Previous studies have used the op-

tical cameras on *HST* to examine bar fractions to $z \sim 1$. In this paper, we use Galaxy Zoo morphological classifications of galaxies imaged by the Cosmic Assembly Near-Infrared Deep Extragalactic Legacy Survey (CANDELS; Grogin et al. 2011; Koekemoer et al. 2011), which uses *HST's* near-infrared Wide-Field Camera 3 (WFC3) to extend the redshift range within which high-resolution rest-frame optical galaxy images are available to $z \gtrsim 2$.

In Section 2 we describe our sample selection, including a summary of Galaxy Zoo classifications of CANDELS galaxies and how disks and bars are selected. We also explore any potential biases that may affect our results. We present our results in Section 3, with a discussion including comparison to simulated predictions in Section 4, and a summary in Section 5. Throughout this paper we use the AB magnitude system, and where necessary we adopt a cosmology consistent with ΛCDM, having $H_0 = 70\mathrm{km\ s^{-1}Mpc^{-1}}$, $\Omega_\mathrm{m} = 0.3$ and $\Omega_\Lambda = 0.7$ (Bennett et al. 2013; Planck Collaboration et al. 2013).

2   DATA

2.1   CANDELS

The Cosmic Assembly Near-infrared Extragalactic Legacy Survey (CANDELS; Grogin et al. 2011) is a *Hubble* Treasury program combining optical and near-infrared imaging from the Advanced Camera for Surveys (ACS) and Wide Field Camera 3 (WFC3) across five well-studied survey fields and at two depths. The wide fields are imaged at 2-3-orbit depths, and the deep fields at $\sim$13-orbit depths, over multiple epochs. These are reduced and combined (a process described in detail by Koekemoer et al. 2011) to produce a single mosaic for each field, with drizzled resolutions of $0''.03$ and $0''.06$ per pixel for ACS and WFC3/IR, respectively.

Here we use the CANDELS ACS and WFC3 images from within the COSMOS, GOODS-South, and UDS fields, for which raw classifications from the Galaxy Zoo project are presently available. The WFC3/IR observations of these fields cover approximately 0.3 square degrees combined. The Galaxy Zoo classifications are based on colour images of 49,555 sources, created using an asinh stretch (Lupton et al. 2004) with WFC3 F160W, F125W, and ACS F814W as red, green and blue respectively.

2.2   Classifications

Galaxy Zoo provides quantified visual morphologies by obtaining multiple independent classifications for each galaxy. Beginning in 2007, more than 1,000,000 galaxy images total from both the Sloan Digital Sky Survey and the *Hubble Space Telescope* have each been classified by typically ~ 40 independent volunteers via a web interface[1]. The initial version of the project (Lintott et al. 2008, 2011) asked a single question per galaxy; subsequent versions have collected more detailed morphological information, including finer sub-structures of disk galaxies such as bulge strength and bars, via a tiered classification tree (e.g., Willett et al. 2013; Melvin et al. 2013).
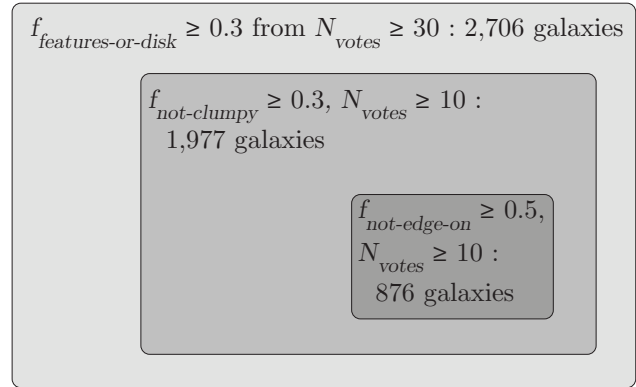
Figure 1. Selection of the featured, not-edge-on disk galaxy sample (876 galaxies) in Galaxy Zoo-CANDELS, using three nested questions in the Galaxy Zoo classification tree. This selection was made independently of restrictions on redshift or luminosity (a full description of the sample selection is described in Section 2.4). Eight independent classifiers subsequently examined each of the 876 disk galaxies for evidence of a bar.

This work uses classifications collected during the fourth release of Galaxy Zoo, specifically 49,555 images from the COSMOS, GOODS-South, and UDS fields in the CANDELS survey (hereafter GZ-CANDELS). The dataset was composed of all sources having $F160W$ (H) apparent magnitude < 25.5. Initial analysis after each galaxy had received typically ~ 20 classifications resulted in the early retirement of 1,555 point-like sources and 11,837 faint, low-surface brightness galaxies without resolvable fine features. Although the project is still ongoing, as of the date of this analysis each of the remaining objects has received at least 40 independent classifications.

The classification tree used for GZ-CANDELS first asks volunteers to choose whether a galaxy is mostly smooth, has features, or is a star/artifact. The bar classification question ("Is there a sign of a bar feature through the centre of the galaxy?") is reached once a volunteer has chosen "Features or Disk" as an answer to the first question and has subsequently said the galaxy does *not* have a mostly clumpy appearance, nor is it an edge-on disk. The bar vote is therefore a fourth-tier question, and the number of volunteers per galaxy who answer the question varies depending on each volunteer's answers to the earlier questions about the galaxy.

2.3   Redshifts

Each of the fields covered by CANDELS data has considerable ancillary data from previous and ongoing work. We assemble photometric and spectroscopic redshifts from the available literature. In COSMOS, we combine spectroscopic and photometric redshifts from the zCOSMOS project (**?**) with photometric redshifts from the NEWFIRM medium-band survey (Whitaker et al. 2011). In GOODS-South, we use the catalog of Cardamone et al. (2010), who compiled available spectroscopic redshifts from multiple sources, to which they added photometric redshifts based on deep broad- and medium-band data from MuSYC (Gawiser et al. 2006). In UDS, we use available spectroscopic (**???**) and photometric (**?**) redshifts, the latter of which make use of

deep multi-wavelength coverage from UKIDSS as well as J and H-band magnitudes from CANDELS (similar to photometric redshifts calculated by, e.g., **?**). Of the 49,555 galaxies originally included in Galaxy Zoo-CANDELS, 46,234 currently have spectroscopic (2,886) or photometric (43,348) redshifts.

2.4 Sample Selection

A full reduction of the GZ-CANDELS classifications, resulting in a catalog of morphological vote fractions for each galaxy, is ongoing. Here we use the raw vote fractions, which have been neither weighted nor debiased (e.g., by a procedure similar to Willett et al. 2013). The effects of using raw versus the reduced classifications are twofold. First, the unweighted vote fractions are likely biased in the first question toward an excess of votes for "Star or Artifact". Second, the effects of surface brightness dimming are not accounted for in the vote fractions, which is potentially a significant effect in a sample extending to $z \sim 2$ in the rest-frame optical.

To minimize the impact of the lack of user weighting, we employ a lower vote fraction threshold when selecting "featured" galaxies compared to thresholds using weighted data. We select as "featured" galaxies those where at least 30% of votes (out of at least 30 volunteers total) were registered for "Features or Disk". This selects 2,706 featured galaxies. After the first question, the user weighting used by previous Galaxy Zoo data reductions affects vote fractions by typically no more than a few percent; we therefore expect the lack of weighting to have little to no systematic effect on additional vote fractions.

Subsequent to the featured galaxy selection, we select a sub-sample where at least 30% of volunteers (of at least 10 who answered the question) registered a vote for "no" to the question "Does the galaxy have a mostly clumpy appearance?" in order to remove galaxies whose features do not clearly include a disk; this selection removes 729 clumpy galaxies in total. We include this selection in order to consider each branch of the classification tree that leads to the bar-feature question, but note that, were we to ignore the clump-threshold criterion completely, this would only cause contamination of the final "featured" sample at the 1% level; our qualitative results are not sensitive to the specific choice of clumpy threshold between $0.1 \leqslant f_{not-clumpy} \leqslant 0.6$.

Further, we also require that 50% of volunteers (of at least 10) registered a vote for not-edge-on. This selects a sample of 876 featured disk galaxies from which a bar may be identified, if it exists. Figure 1 shows a visual representation of this sample selection, from which a further sub-sample of barred galaxies may be identified. However, approximately 20% of these 876 galaxies received less than 10 raw votes *total* for the question "Is there any sign of a bar feature through the centre of the galaxy?", a consequence of the broad initial selection of featured galaxies and the multiply-branched nature of the classification tree. Because of the lower number of votes per galaxy in the 4th tier of the classification tree (the position of the bar question), within the featured sample the raw bar fractional vote is statistically useful, but uncertain for individual galaxies.

We therefore elected to use internal visual classifications from the Galaxy Zoo science team to select the sub-sample of barred disk galaxies. Eight of the authors inspected each
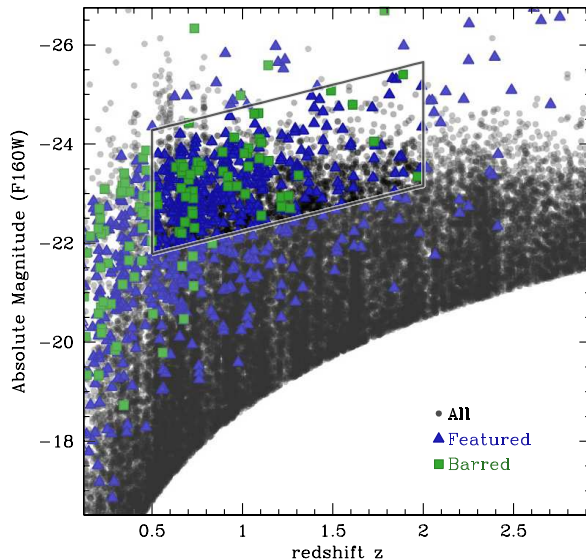

Figure 3. Absolute H-band magnitude versus redshift for all sources (gray/black circles), 876 "Featured" not-edge-on disks (blue triangles), of which 123 galaxies show clear evidence of a bar (green squares). To facilitate comparison between lookback times, avoid biases due to surface-brightness dimming when calculating bar fractions, and ensure all observed H-band flux is redward of the 4000-Å break, we select sub-samples within the same region of the evolving galaxy luminosity function (Marchesini et al. 2012) and $0.5 \leqslant z \leqslant 2$ (parallelogram). Within this region there are 370 not-edge-on disk galaxies, 56 of which have clear evidence of bars.

of the 876 featured disk galaxies for evidence of a bar; these votes were unanimous approximately 60% of the time, for either a bar feature (23 galaxies) or no bar (512 galaxies). Following vote fraction thresholds used in previous studies (Masters et al. 2011; Melvin et al. 2013), we mark a galaxy as barred if at least half of classifiers indicated the presence of a bar. The absolute H-band magnitudes of these galaxies are plotted as a function of redshift in Figure 3. Of the featured not-edge-on (and barred) galaxies, 525 (61) have redshifts between $0.5 \leqslant z \leqslant 2.0$. Within this redshift range, all flux collected by the WFC3 H band is redward of the 4000-Å break. Examples of barred and unbarred galaxies are shown in Figure 2.

To minimize the biasing caused by surface-brightness dimming at higher redshifts, we additionally employ a conservative luminosity cut when examining bar fractions, choosing a minimum H absolute magnitude of -23.15 at $z = 2$ (or approximately an apparent $H = 23.5$). This ensures that featured galaxies can be detected within the sub-sample at all $z < 2$. We note that this is brighter than the knee of the rest-frame-V-band luminosity function at this redshift (Marchesini et al. 2012). In order to examine similar populations across our entire redshift range, we choose a varying luminosity cut based on selecting the same region of the evolving luminosity function (corrected to observed H band; Blanton & Roweis 2007; Marchesini et al. 2012): this selection is shown as a parallelogram shape in Figure 3. This final cut produces 370 featured, not-edge-on galaxies, of which 56 have strong bar signatures. We note that
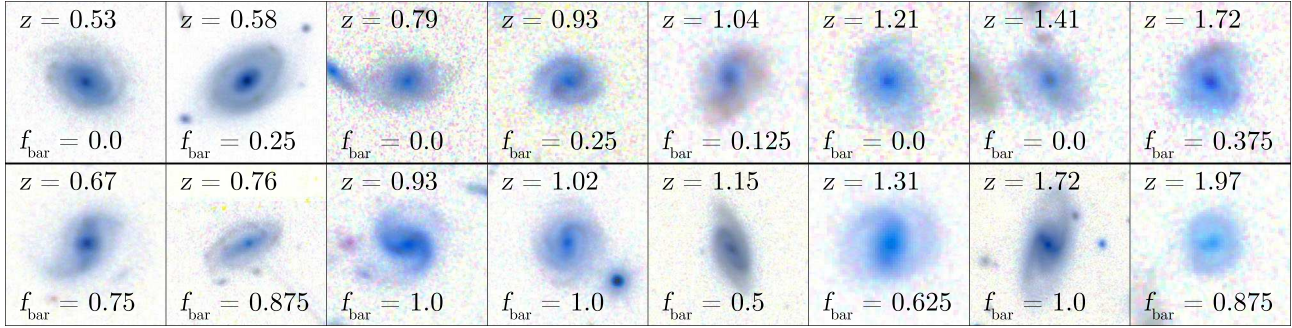
$z = 0.53$	$z = 0.58$	$z = 0.79$	$z = 0.93$	$z = 1.04$	$z = 1.21$	$z = 1.41$	$z = 1.72$
$f_{\mathrm{bar}} = 0.0$	$f_{\mathrm{bar}} = 0.25$	$f_{\mathrm{bar}} = 0.0$	$f_{\mathrm{bar}} = 0.25$	$f_{\mathrm{bar}} = 0.125$	$f_{\mathrm{bar}} = 0.0$	$f_{\mathrm{bar}} = 0.0$	$f_{\mathrm{bar}} = 0.375$
$z = 0.67$	$z = 0.76$	$z = 0.93$	$z = 1.02$	$z = 1.15$	$z = 1.31$	$z = 1.72$	$z = 1.97$
$f_{\mathrm{bar}} = 0.75$	$f_{\mathrm{bar}} = 0.875$	$f_{\mathrm{bar}} = 1.0$	$f_{\mathrm{bar}} = 1.0$	$f_{\mathrm{bar}} = 0.5$	$f_{\mathrm{bar}} = 0.625$	$f_{\mathrm{bar}} = 1.0$	$f_{\mathrm{bar}} = 0.875$

Figure 2. Examples of featured galaxies in GZ-CANDELS, showing disk galaxies whose bar fraction, f_{bar} were below (top row) and above (bottom row) the threshold for inclusion in the barred sub-sample.

our results are robust to small variations in the redshift and luminosity thresholds chosen for the sample.

3 RESULTS: BAR FRACTIONS

The fraction of disk galaxies with bars between $0.5 \leqslant z \leqslant 2$ is $\sim 10 - 20\%$, independent of any reasonable selection on luminosity ranges or vote fractions for detected features, lack of clumpiness, disk inclination angle, and strong bar features. Figure 5 shows the bar fraction with lookback time, from $t_{lb} = 5.0$ Gyr ($z = 0.5$) to 10.2 Gyr ($z = 2.0$). The sample encompasses the same subset of the galaxy luminosity function relative to the evolving L^*; the conservative selection to ensure detectability of features (or lack thereof) to $z = 2$ means the galaxies examined here are all brighter than L^* at their epoch.

Within this sample, and given the uncertainties, the bar fraction is consistent with zero evolution beyond $z > 1$. Previous studies of the bar fraction at $z \lesssim 1$ generally find that the bar fraction does evolve (Abraham et al. 1996, 1999; Elmegreen et al. 2004; Elmegreen & Elmegreen 2005; Sheth et al. 2008; Cameron et al. 2010; Masters et al. 2011; Melvin et al. 2013, though these findings are not unanimous; Jogee et al. 2004). Although the details depend on both the bar selection method being used and the properties of the galaxies themselves, disk galaxies are more likely to show strong bar features at lower redshift. Two independent studies of the full COSMOS-ACS sample (Sheth et al. 2008; Melvin et al. 2013) show that the fraction of visually identified strong bars decreases with redshift, from approximately 35% at $z = 0.2$ to 15% at $z = 1$.

Figure 5 shows the visually identified strong bar fraction versus redshift in the context of other work, both observational and theoretical. Within the redshift range where we overlap with other observational studies, the bar fraction is consistent. However, the bar fraction evolution appears to flatten at $z > 1$; our result is not consistent with a simple extrapolation of the decreasing bar fraction trend found by other studies.

Using zoom-in cosmological simulations of 33 field and loose group galaxies, Kraljic et al. (2012) find that disk galaxies at $z \gtrsim 1$ are generally too dynamically hot to become unstable to bar formation; this manifests itself as a decreasing bar fraction with redshift. Although the quantitative bar fractions in their simulations depend on the threshold used to define a bar feature, the fraction of disk galaxies
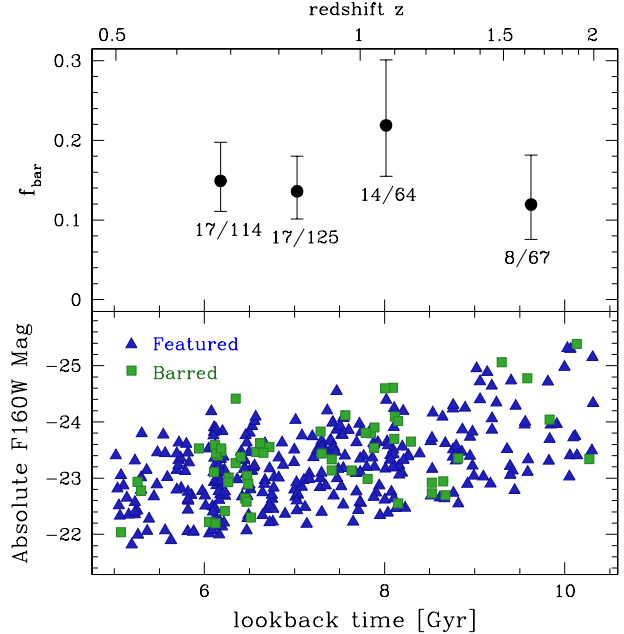

Figure 4. *Top panel:* Bar fraction versus lookback time. Uncertainties are binomial error bars (Gehrels 1986); within these uncertainties, the bar fraction is consistent with no evolution from $0.5 \leqslant z \leqslant 2$. *Bottom panel:* absolute H-band magnitudes of the sample from which the fractions are drawn.

hosting bars drops to zero, or near zero, by any definition they use (Figure 5 shows their standard "strong bar" definition). This initially appears inconsistent with our results showing a low, but non-zero, bar fraction. However, due to the small sample size of Kraljic et al. compared to observational studies, a complete lack of bar feature detection within the subset of their sample identified as disk galaxies is consistent with a bar fraction of $\approx 15\%$ within uncertainties.

We also note that the galaxy masses and luminosities used in the simulations were on average lower than those examined in this work, making a direct comparison to this work more difficult, as bar fraction also depends somewhat on stellar mass. Kraljic et al. predict that massive disk galaxies will be more likely to form bars at higher redshift than lower mass disk galaxies due to higher-mass galaxies reaching dynamical maturity at earlier epochs. This is qualita-
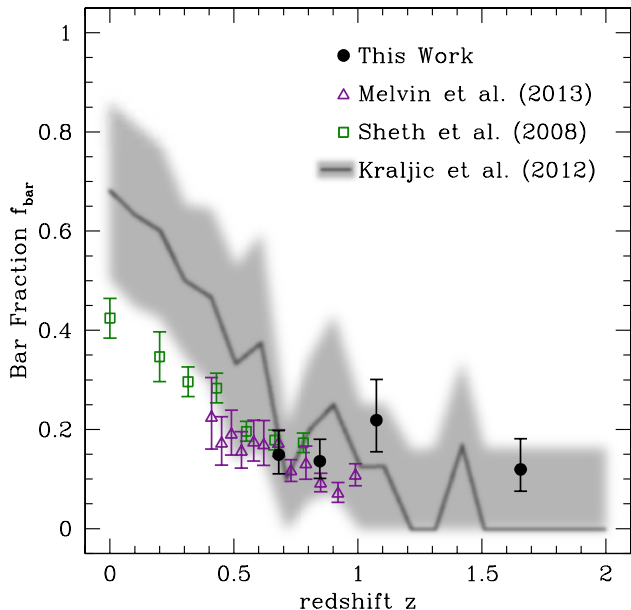
Figure 5. Fraction of disk galaxies having a bar feature versus redshift, in the context of other work. Bar fractions in this work (black circles) at $z < 1$ are generally consistent with those of Sheth et al. (2008, visually identified strong bars; green squares) and Melvin et al. (2013, purple triangles) despite differences in selection methods. Uncertainties in observed and predicted fractions were calculated assuming binomial statistics. Kraljic et al. (2012) computed the fraction of strong bars to $z = 2$ among disk galaxies that evolved to stellar masses $M_* \approx 10^{10-11} \mathrm{M}_\odot$ (shaded region).

tively consistent with our finding that the bar fraction at $z \sim 2$ is approximately $10 - 20\%$ within 1σ binomial uncertainties, but a direct and quantitative theoretical comparison to our observational result is currently not possible given available simulations.

Our results agree with the consensus reached by previous work that the epoch of bar formation (and thus disk dynamical maturity) begins at $z < 1$. However, bars are not completely absent even at $z \sim 2$: some fraction of disks at the masses probed by our sample are mature enough even by this epoch ($\sim 3 - 4$ Gyr after the Big Bang) to host a bar.

The incidence of bars among massive disks may be due at least in part to galaxy mergers. Minor galaxy mergers may dynamically heat a disk and destroy a bar, or they may trigger the formation of a bar, depending on the particulars of the interaction (Gerin et al. 1990; Berentzen et al. 2003, 2004; **?**). The relative likelihood of these contrasting end results, combined with the incidence of minor mergers among this population at $z \sim 2$, may combine to produce a net effect that stabilizes the bar fraction at $z \sim 10\%$ during this epoch of galaxy assembly.

4 SUMMARY

Using visual classifications of rest-frame optical *HST* galaxy images from the ongoing Galaxy Zoo-CANDELS project, we examined for the first time the fraction of disk galaxies

hosting a bar feature to $z \sim 2$ in order to trace the dynamical stability of disks as early as ~ 3 Gyr after the Big Bang. We find that the bar fraction to $z \sim 1$ is consistent with previous studies using similar analysis methods.

At $z > 1$, the bar fraction is approximately $10 - 20\%$ and consistent with no evolution between $1 < z < 2$. This is qualitatively consistent with the predictions of zoom-in cosmological simulations, although further work is needed to determine whether simulations of disk galaxies with $L > L^*$ predict the same quantitative strong bar fraction at $z < 2$.

That the bar fraction from $1 < z < 2$ appears to be small but constant among massive disk galaxies implies that massive disk dynamics do not rapidly change on average over this period. Further clarification may come in the future when additional detailed morphological classifications of deep $z \sim 2$ rest-frame optical galaxy images are available; additional simulations will help provide a more nuanced understanding of the underlying physical causes of this apparently stable bar fraction.

REFERENCES

Abraham R. G., Merrifield M. R., Ellis R. S., Tanvir N. R., Brinchmann J., 1999, MNRAS, 308, 569

Abraham R. G., Tanvir N. R., Santiago B. X., Ellis R. S., Glazebrook K., van den Bergh S., 1996, MNRAS, 279, L47

Aguerri J. A. L., Mndez-Abreu J., Corsini E. M., 2009, A&A, 495, 491504

Athanassoula E., 2005, Celest.Mech.Dyn.Astron.

Athanassoula E., Machado R. E. G., Rodionov S. A., 2013, MNRAS, 460

Bennett C. L. et al., 2013, ApJS, 208, 20

Berentzen I., Athanassoula E., Heller C. H., Fricke K. J., 2003, MNRAS, 341, 343

Berentzen I., Athanassoula E., Heller C. H., Fricke K. J., 2004, MNRAS, 347, 220

Berentzen I., Shlosman I., Martinez-Valpuesta I., Heller C. H., 2007, ApJ, 666, 189200

Blanton M. R., Roweis S., 2007, AJ, 133, 734

Cameron E. et al., 2010, MNRAS, 409, 346

Cardamone C. N. et al., 2010, ApJS, 189, 270

Combes F., 2009, in Astronomical Society of the Pacific Conference Series, Vol. 419, Galaxy Evolution: Emerging Insights and Future Challenges, Jogee S., Marinova I., Hao L., Blanc G. A., eds., p. 31

Conselice C. J., Bershady M. A., Dickinson M., Papovich C., 2003, Astron.J., 126, 1183

Darg D. W. et al., 2010a, MNRAS, 401, 1552

Darg D. W. et al., 2010b, MNRAS, 401, 1043

Elmegreen B. G., Elmegreen D. M., 2005, ApJ, 627, 632

Elmegreen B. G., Elmegreen D. M., Hirst A. C., 2004, ApJ, 612, 191

Friedli D., Benz W., 1993, A&A, 268, 6585

Gawiser E. et al., 2006, ApJS, 162, 1

Gehrels N., 1986, ApJ, 303, 336

Gerin M., Combes F., Athanassoula E., 1990, A&A, 230, 37

Grogin N. A. et al., 2011, ApJS, 197, 35

Jogee S. et al., 2004, ApJ, 615, L105

Koekemoer A. M. et al., 2011, ApJS, 197, 36

Kraljic K., Bournaud F., Martig M., 2012, ArXiv e-prints, 1207.0351

Lilly S. J., Le Fevre O., Hammer F., Crampton D., 1996, ApJ, 460, L1

Lintott C. et al., 2011, MNRAS, 410, 166

Lintott C. J. et al., 2008, MNRAS, 389, 1179

Lotz J. M., Jonsson P., Cox T., Croton D., Primack J. R., et al., 2011, Astrophys.J., 742, 103

Lupton R., Blanton M. R., Fekete G., Hogg D. W., O'Mullane W., Szalay A., Wherry N., 2004, PASP, 116, 133

Madau P., Pozzetti L., Dickinson M., 1998, ApJ, 498, 106

Marchesini D., Stefanon M., Brammer G. B., Whitaker K. E., 2012, ApJ, 748, 126

Masters K. L. et al., 2012, MNRAS, 424, 2180

Masters K. L. et al., 2011, MNRAS, 411, 2026

Melvin T., et al., 2013, submitted to MNRAS

Moore B., Katz N., Lake G., Dressler A., Oemler A., 1996, Nature, 379, 613616

Nair P. B., Abraham R. G., 2010, ApJL, 714, L260L264

Planck Collaboration et al., 2013, ArXiv e-prints, 1303.5076

Sellwood J. A., 2010, ArXiv e-prints, 1006.4855

Sheth K. et al., 2008, ApJ, 675, 1141

Skibba R. A. et al., 2012, MNRAS, 423, 1485

Taylor M. B., 2005, in Astronomical Society of the Pacific Conference Series, Vol. 347, Astronomical Data Analysis Software and Systems XIV, Shopbell P., Britton M., Ebert R., eds., p. 29

Villa-Vargas J., Shlosman I., Heller C., 2010, ApJ, 719, 14701480

Whitaker K. E. et al., 2011, ApJ, 735, 86

Willett K. W. et al., 2013, ArXiv e-prints, 1308.3496

Wright E. L., 2006, PASP, 118, 1711

APPENDIX A: POSSIBLE SOURCES OF ERROR IN BAR FRACTIONS

There are several potential sources of error that could affect our results. Below we address these and discuss their potential impact on the results presented here.

• *Missing disk galaxies:* as disks with an exponential light profile fall below the noise limit more quickly as a function of redshift than more concentrated bulges, it is possible that a study could preferentially miss disks at high redshift. This motivated the conservative lower luminosity limit (Section 2.4). Additionally, we have chosen to sample the same part of the galaxy luminosity function (relative to the evolving knee) across our redshift range, which minimizes the loss of disk galaxies in the lower-redshift part of the sample compared to a luminosity-limited approach that samples brighter, rarer galaxies compared to the bulk of the population as the sample redshift decreases. For both of these reasons as well as the depth of the CANDELS images it is likely that the underlying sample selection does not bias against detection of disk galaxies.

Additionally, our relatively broad selection of galaxies with "Features or Disk" within Galaxy Zoo is designed to account for the systematic downward shift of unweighted vote fractions that have not been corrected for (in particular) errant "Star or Artifact" selections. Accounting for this in the first morphological selection prevents it from systematically affecting the rest of the classifications, as errant selections are removed from the rest of the classification tree so do not affect further branches. We also note that the bar fraction results discussed in Section 3 are not strongly dependent on any choice of the vote threshold for features between $0.25 \leqslant f_{feat} \leqslant 0.5$.

• *Missing bars within featured galaxies:* a bar feature creates a linear excess of surface brightness, so if disk galaxies as a whole are well detected in a rest-frame optical sample, bars are not likely to be missed. For examination of bar fractions, we have chosen the upper redshift limit of $z < 2$ specifically so that the H band is fully in the rest-frame optical, redward of the 4000-Å break; although some bars are detected at higher redshifts, this limit is conservative in terms of completeness for bar fraction studies.

Additionally, using Galaxy Zoo classifications is demonstrably reliable for selection of specific features (Darg et al. 2010b,a; Masters et al. 2011; Skibba et al. 2012; Willett et al. 2013; Melvin et al. 2013; **?**). The requirement that at least 50% of classifiers vote for a bar feature is most closely related to what other selection methods call a *strong* bar (**?**Nair & Abraham 2010); weaker bars may be present in the sample, and statistically speaking the bar vote fraction tracks

bar strength, even among "experts" – but, of course, contamination becomes an issue for lower thresholds. By using expert follow-up classifications we minimize contamination in the higher-tiered branch of the question tree currently affected by low-number statistics and the compounded effects of lack of classification weighting and debiasing, and we have chosen a vote threshold to provide a roughly similar selection to other studies for ease of comparison. However, we note that there may be weaker bar instabilities present but not included in our barred sample.

• *Redshift errors:* The majority of redshifts in our sample are photometric, not spectroscopic, which has the advantage of being complete even for high-redshift samples where emission lines are difficult to detect in spectra, but redshift biases are a concern. However, a simple monte carlo approach varying the photometric redshifts within their reported uncertainties does not affect the statistical results in the sample. In part, this is because many of the photometric redshifts are based on medium-band photometry (Cardamone et al. 2010; Whitaker et al. 2011; **?**), which is very reliable (**some stats here**).

• *Others?*